Electronic Supplementary Material (ESI) for Nanoscale.

Formation of Fe_3O_4@SiO_2@C/Ni Hybrids with Enhanced Catalytic Activity and Histidine-rich Protein Separation

Yanwei Zhang[a], Min Zhang*[,a], Jinbo Yang[a], Lei Ding[a], Jing Zheng[a], Jingli Xu*[,a], and Shenglin Xiong*[,b]

[a]College of Chemistry and Chemical Engineering, Shanghai University of Engineering Science, Shanghai 201620, PR China.

[b]Key Laboratory of the Colloid and Interface Chemistry, Ministry of Education, and School of Chemistry and Chemical Engineering, Shandong University, Jinan, 250100, PR China

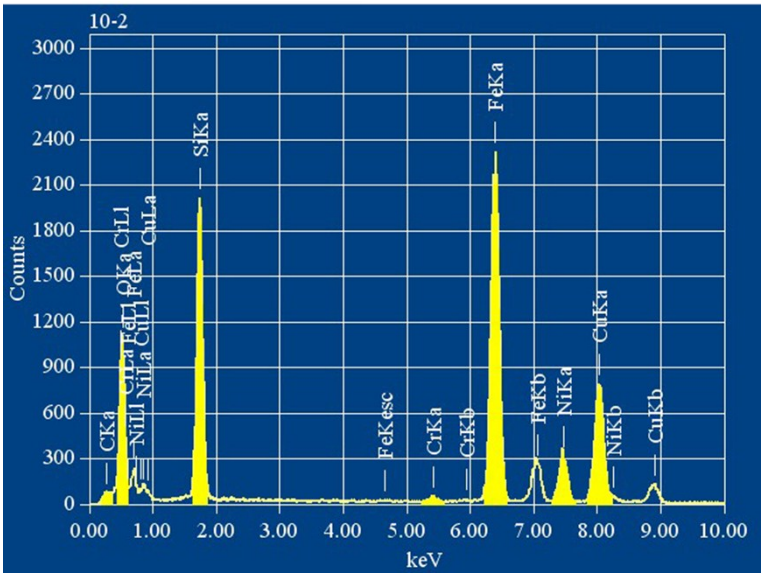

Figure S1. Energy-disperse X-ray spectrum (EDS) of Fe_3O_4@SiO_2@C/Ni-1 composites

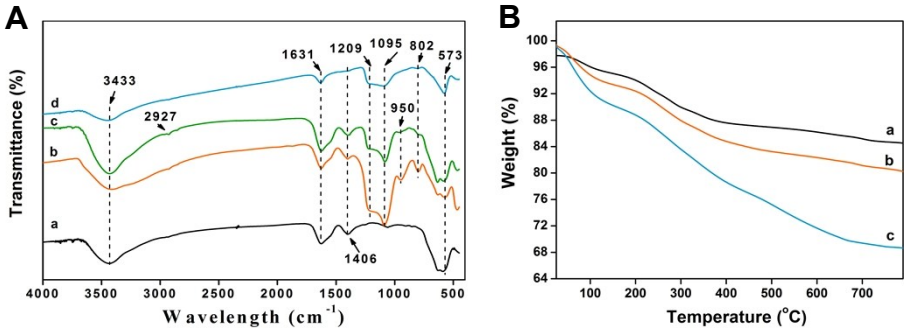

Figure S2. (A) FTIR spectra of Fe_3O_4 (a), Fe_3O_4@SiO_2 (b), Fe_3O_4@SiO_2@PDA-Ni^{2+}-1 (c) and Fe_3O_4@SiO_2@C/Ni-1 (d). **(B)** TGA test of Fe_3O_4@SiO_2 (a), Fe_3O_4@SiO_2@PDA-Ni^{2+}-1 (b), Fe_3O_4@SiO_2@PDA-Ni^{2+}-2 (c).

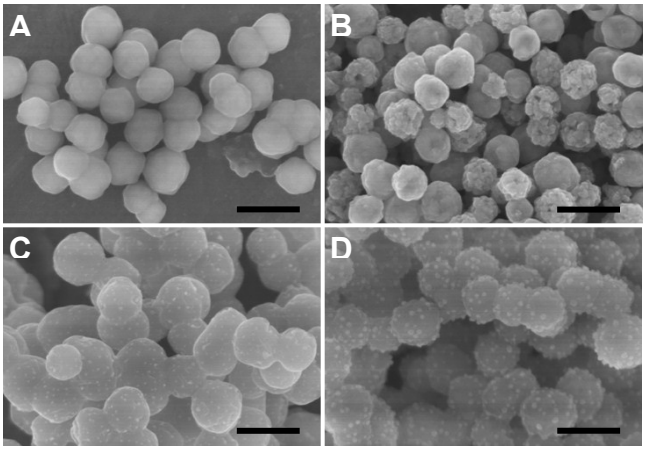

Figure S3. FESEM images of products obtained by annealing Fe_3O_4@SiO_2@PDA-Ni^{2+}-1 under N_2 atmosphere at 350 °C (A), 600 °C (C); FESEM images of core-shell structured Fe_3O_4@SiO_2@C/Ni composites obtained by annealing Fe_3O_4@SiO_2@PDA-Ni^{2+}-2 under N_2 atmosphere at 350°C (B), 600°C (D). Scale bars: 500 nm (**A**-**D**).

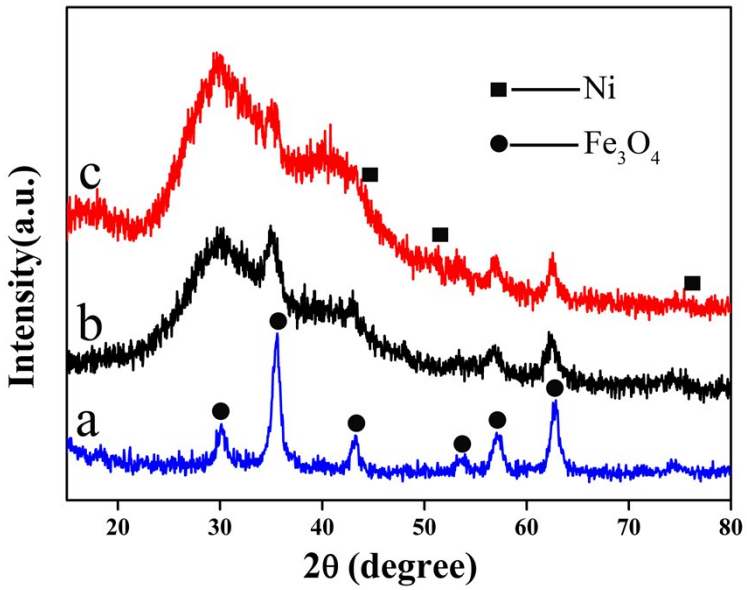

Figure S4. XRD patterns of Fe_3O_4 (a), Fe_3O_4@PDA/Ni^{2+} (b), Fe_xO_y@C/Ni(c) (($M_{dopamine:nickel}$ of 1:2, 37.6 mg nickel salt and 15 mg dopamine, carbonization at 500°C)

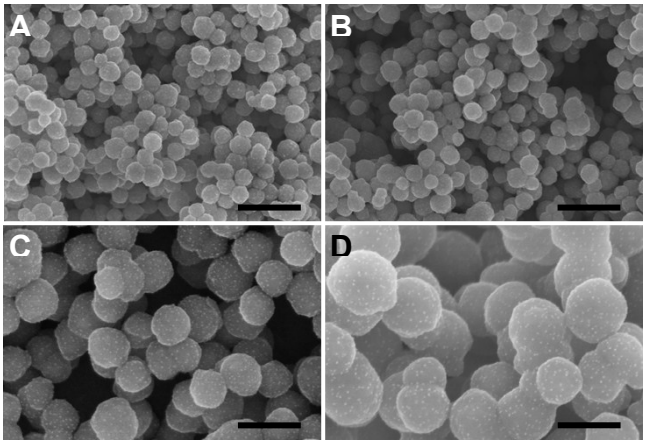

Figure S5. FESEM of Fe_3O_4@SiO_2@C/Ni with different thickness of SiO_2 by adjusting the different amount of TEOS from 50 μL (a), 150 μL (b), 300 μL (c), 500 μL (d) while keeping the other parameters fixed. Scale bars: 500 nm (**A, C**) and 250 nm (**B, D**).

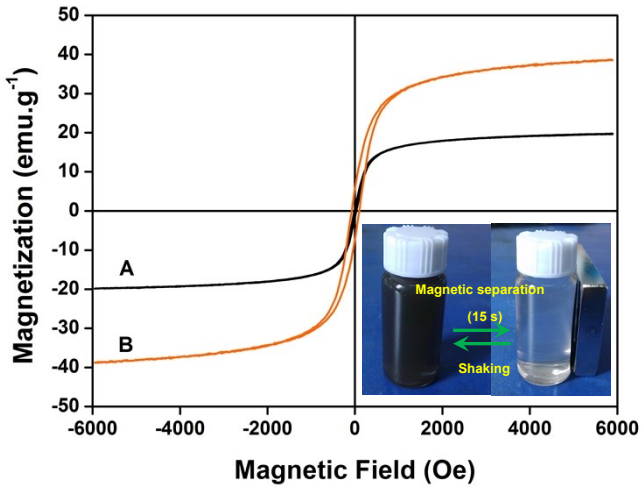

Figure S6. Magnetic hysteresis curves of Fe_3O_4@SiO_2@PDA-Ni^{2+}-1 (A), Fe_3O_4@SiO_2@C/Ni-1 (B) measured at room temperature. (the inset is the digital picture showing that Fe_3O_4@SiO_2@C/-1 can be isolated from the solution by magnet.)

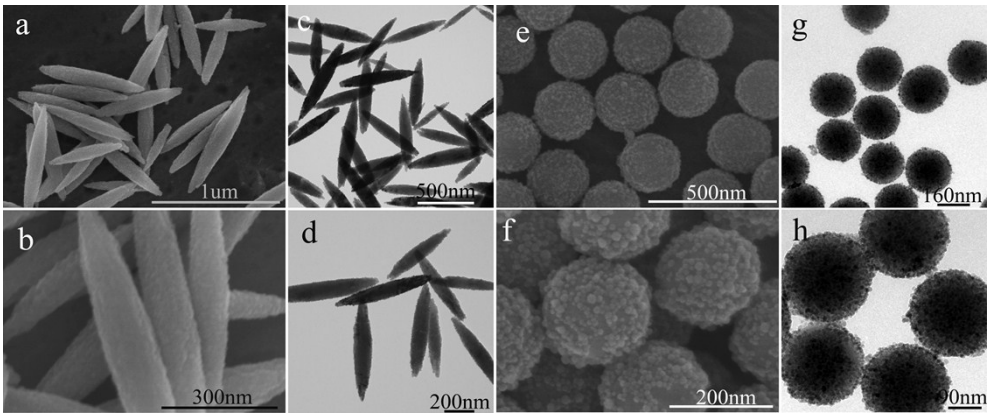

Figure S7. SEM and TEM images of α-Fe_2O_3 (a-d) and SiO_2@Fe_3O_4 (e-h).

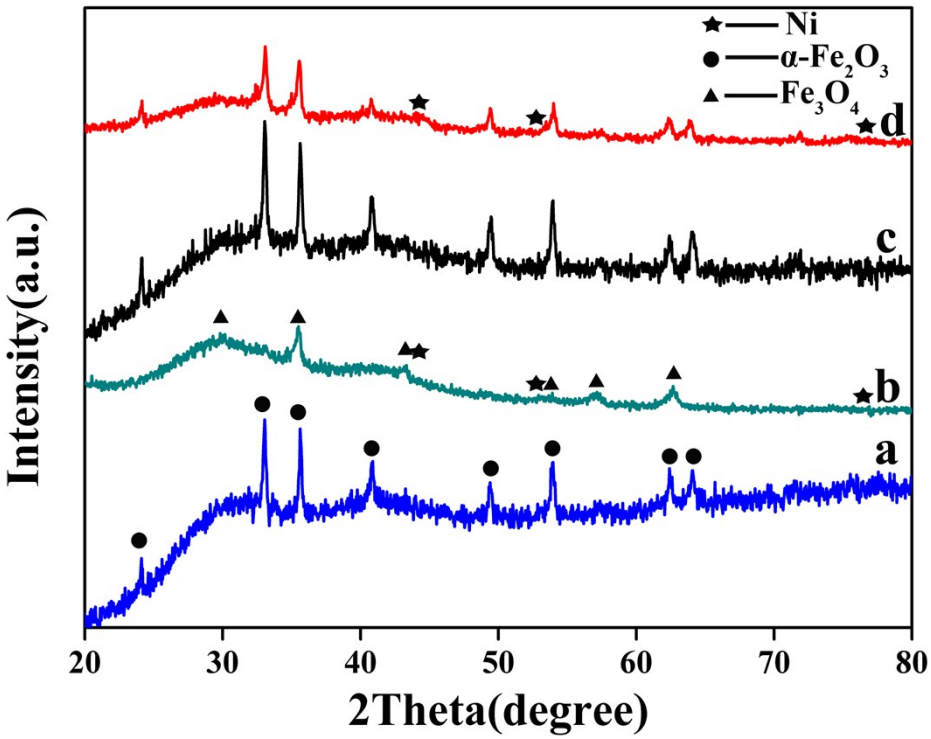

Figure S8. XRD patterns of α-Fe_2O_3@PDA/Ni^{2+} (a), Fe_3O_4@C/Ni (b), α-Fe_2O_3@SiO_2@PDA/Ni^{2+} (c) and α-Fe_2O_3@SiO_2@C/Ni (d).

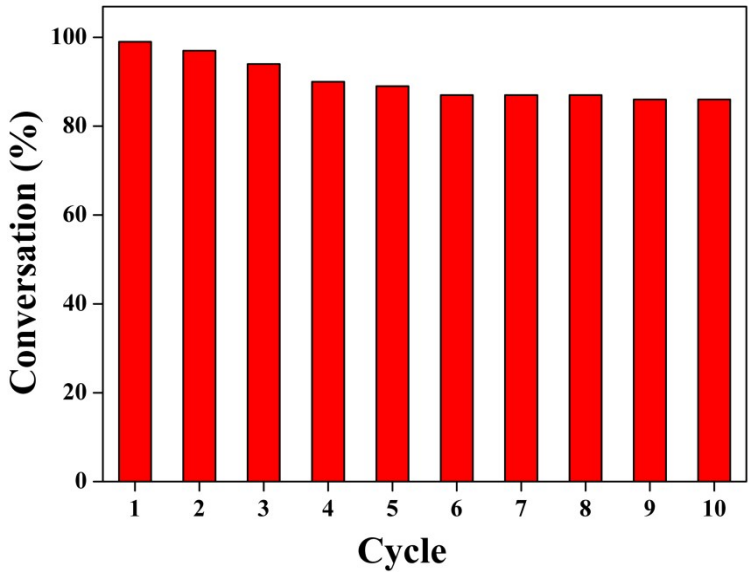

Figure S9. Recyclability of Fe_3O_4@SiO_2@C-Ni-1 as Catalysts for the reduction of 4-nitrophenol.

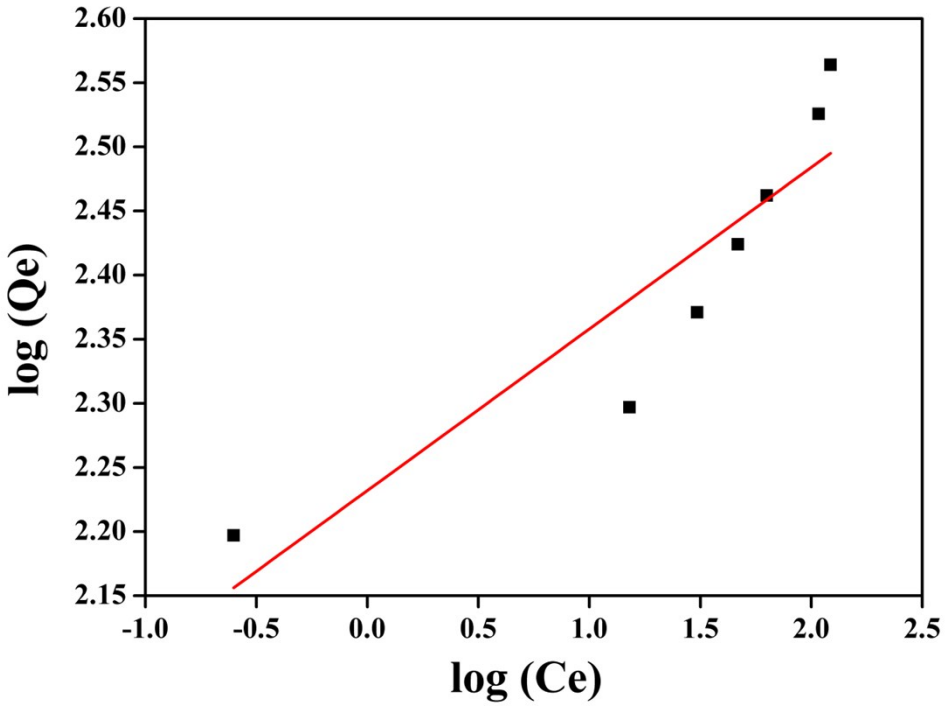

Figure S10. Linear fitting of adsorption isotherms plots based on Freundlich model.

Table S1 the estimate of Langmuir model and Freundlich model

Langmuir			Freundlich		
Q_m	b	R^2	K_F	n	R^2
409.84	0.045	0.996	170.63	7.94	0.7884

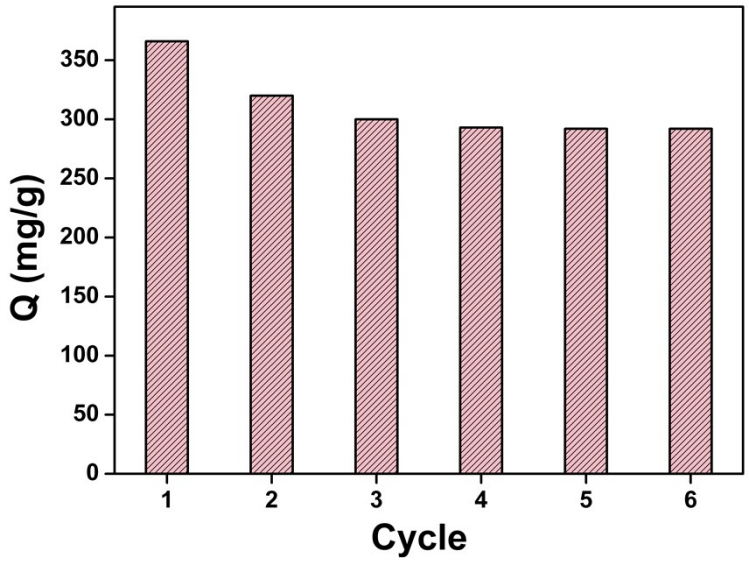

Figure S11. Reusability of Fe_3O_4@SiO_2@C/Ni-1 through the adsorption–regeneration cycle.

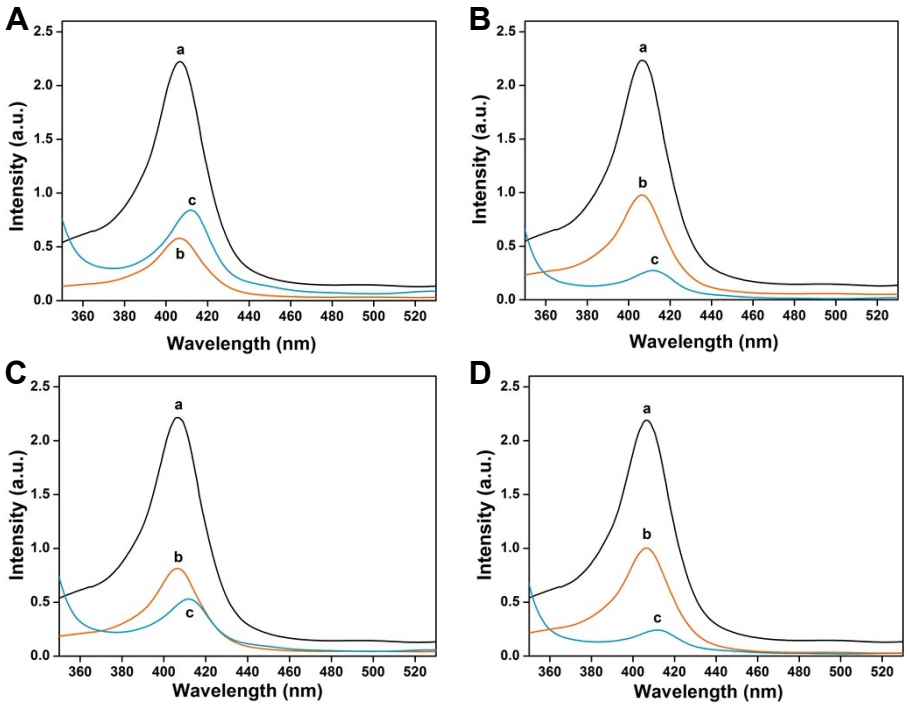

Figure S12. (A) Curve a is UV-vis spectra of initial BHb (A), BHb/BSA binary solution (B), BHb/Lysozyme binary solution (C), BHb/BSA/Lysozyme ternary solution(D). Curve b is UV-vis spectra of supernatant of BHb (A), BHb/BSA binary solution (B), BHb/Lysozyme binary solution (C), BHb/BSA/Lysozyme ternary solution (D) after adsorbed by Fe_3O_4@SiO_2@C/Ni-1 Curve c is UV-vis spectra of desorption solution of Fe_3O_4@SiO_2@C/Ni-1 in BHb (A), BHb/BSA binary solution (B), BHb/Lysozyme binary solution (C), BHb/BSA/Lysozyme ternary solution (D) with 0.2 g mL^{-1} imidazole solution as the eluent.

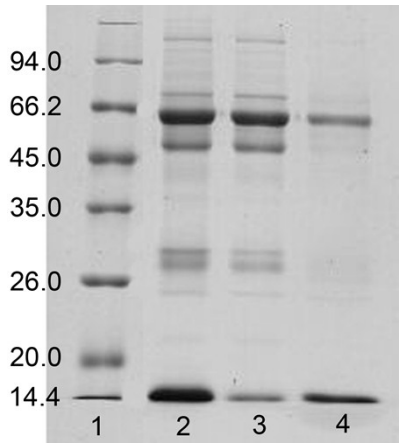

Figure S13. SDS-PAGE analysis of adsorption by Fe_3O_4@SiO_2@C/Ni-1 from solution. Lane 1, marker; lane 2, initial human blood diluted 60-fold as the control; lane 3, residual human blood solution after adsorption by Fe_3O_4@SiO_2@C/Ni-1; lane 4, the eluted human blood from Fe_3O_4@SiO_2@C/Ni-1 by 0.2 g ml^{-1} imidazole solution.